ISSN: 2594 - 2905

TEMPERATURE PROTECTION OF SUBMERSIBLE PUMP MOTOR WINDINGS

PROTECTION TEMPERATURE PROTECTION OF SUBMERSIBLE PUMP MOTOR WINDINGS

Oscar Manuel Cortés[1], Mario Salvador Esparza-González [2], Christian Geovanni Hernández-Murillo[3]

https://doi.org/10.61117/ipsumtec.v7i2.312

[1]Master of Science in Electrical Engineering. Tecnológico Nacional de México / Instituto Tecnológico de Aguascalientes, Department of Electrical and Electronic Engineering. R24153076@aguascalientes.tecnm.mx, 449 199 4934, Av. Adolfo López Mateos #1801 Ote. Fracc. Bona Gens, C.P. 20256 Aguascalientes, Ags. https://orcid.org/0009-0008-8748-842X.
[2]Master of Science in Electrical Engineering. Tecnológico Nacional de México / Instituto Tecnológico de Aguascalientes, Department of Electrical and Electronic Engineering. mario.eg@aguascalientes.tecnm.mx, 449 256 0982, Av. Adolfo López Mateos #1801 Ote. Fracc. Bona Gens, C.P. 20256 Aguascalientes, Ags. https://orcid.org/0009-0000-8837-5525.
[3]Doctorate in Engineering Sciences. Tecnológico Nacional de México / Instituto Tecnológico de Aguascalientes, Department of Electrical and Electronic Engineering. christian.hm@aguascalientes.tecnm.mx, 449 254 77 59, Av. Adolfo López Mateos #1801 Ote. Fracc. Bona Gens, C.P. 20256 Aguascalientes, Ags. https://orcid.org/0009-0003-4406-245X.

Abstract -- In this research work a protection is presented that is placed in the windings of the submersible pump motor to detect its temperature, when it increases to a value higher than 75 °C, it generates a signal with a frequency of 200kHz which is sent through the power cables to a receiver in the motor starter.

The design includes the power supply, a current carrier transmitter based on a Voltage Controlled Oscillator (VCO), to detect the signal a Phase Locked Loop (PLL) is used as a receiver, these circuits are isolated on the power line by a pair of high voltage capacitors and an intermediate frequency transformer (IFT).

The protection was tested by separating the transmitter and receiver at a distance of 13.5 m. The temperature comparator handles a hysteresis range of 70.47 to 75 °C.

Key words: Protection, windings, transmitter, receiver, current carrier.

***Abstract**:* In this investigation work a protection is presented that is placed in those reeled of the motor of submersible pump for detecting its temperature and when it detects that it is increased to a superior value to the 75°C, it generates a sing with a frequency of 200 kHz which is a correspondent through the feeding cables until a receiver in the starter of the motor.

The design includes the feeding source, a transmitter for carrier current based on a VCO (Voltage Controlled Oscillator), to detect the sing we use a PLL (Phase- Locked Loop) as receiver, these circuits are isolated of the feeding line by means of a couple of capacitors of high voltage and a transformer of intermediate frequency (TFI).

The system was proven separating the transmitter and the receiver a distance of 13.5 m, the comparative of temperature manages a hysteresis range from the 70.47 to the 75 °C.

Key words: Protection, reeled, transmitter, receiver, carrier current.

INTRODUCTION

Three-phase induction motors (MITs) are widely used in industry, they are the workhorse of the industrial sector, due to their almost zero maintenance, in addition to the fact that they exist in a wide range of sizes and capacities [1].

A special case are the MITs for submersible pumps (MBS), which [2] considers vital and mentions that can be used in various applications, such as large-scale water conservation projects [3], urban water supply [4], drainage systems [5], mine drainage [6], emergency disaster relief [7] and other applications. That is why there is a concern to analyze their behavior and maintain them in optimal conditions for their correct operation. There are two main differences between this type of MBS and the dry type, the main one is that the windings of the MIT for submersible pumps are in permanent contact with the pumped liquid, for this same reason, the other difference is that they are wound with magnet wire coated (AMP) with a thermoplastic insulator, while the dry type MIT use varnished magnet wire.

MBS failures can be mechanical and electrical. Mechanical failures have the particularity that their evolution is relatively slow; on the contrary, electrical failures generally present a fast evolution until becoming a catastrophic failure in a short time [8], therefore, their

detection is often very difficult and early detection is essential [9].
Specifically stator winding failures are one of the main failures in MBS, in the work done by [10] reviewed and discussed the failures or malfunctions of electrical submersible pumps (ESP). Therefore, he reviewed all the important information related to this machine, such as construction and operation. He specifically focused on the failures and the details of the . For this, he defines failure as the change in any component of the machine that prevents its proper operation. It can also be defined as the unavailability of an element to perform an intended action. The review arrived at the result that motor failure contributes 40% of all total system failures. In the context of motor failure, stator winding and bearing failures are responsible for about 35 to 40% of total motor failures each. It is notable that many motor failures are related to mechanical failures that result in an increase motor temperature, thereby causing a breakdown of the insulation and this in turn, a short circuit.

In [11] defines an electrical insulator as a medium or material that, when placed between conductors at different potentials, allows only a small or negligible current to flow through it in phase with the applied voltage, the range of resistivities of substances that can be considered insulators goes from more than $10^{20}$to about 10($^{(6)\ \Omega cm}$, depending on the application and the voltage stress, , it defines the dielectric strength or resistance of an insulation as the maximum voltage per unit thickness that a dielectric can withstand in a uniform field before breaking electrically. Dielectric strength is usually measured in kilovolts per millimeter or per inch.

Proper fault identification is time consuming and requires highly trained human experts, and after implementation, monitoring is restricted to the acquisition of some basic parameters, such as current consumption. This scenario emphasizes the need to diagnose faults even before purchasing the equipment, in [12] an artificial intelligence solution is presented to diagnose faults before the acquisition submersible oil motor pump systems.

To validate their proposal and select the best classifier they conducted a comparative study using thousands of real data inputs acquired in tests performed prior to the acquisition of submersible motor pumps, the results showed that the performance of the classifiers is sufficient to facilitate the work performed by humans and, consequently, reduce the time spent in the pump fault diagnosis process. They concluded that, although the system has been evaluated with real data and real test scenarios, there is still a need to investigate the performance of the classifiers when considering sensor data sets rather than individual sensor data.

By investigating numerous submersible motor pumps from various manufacturers in various wells in Egypt [13] it was found that most of the submersible motor failures were caused by excessive motor heating, the researcher offers protection by using three thermometer sensors placed in the motor winding and sending a signal to a microcontroller connected in series with the inverter. The simulation results agree reasonably well with those measured experimentally for the motor used in the research. They concluded that the proposed scheme is simple and economical, while being highly efficient, giving high accuracy and suggest that company producers install sensors inside submersible motors to protect them against overheating.

In another work presented by [14], they propose a deep belief network (DBN)-based fault diagnosis method that can automatically extract the fault characteristic information from the original operating data of a submersible reciprocating pumping unit (SRPU). The operating current is used as the characteristic parameter of the operating state of the SRPU. The vector extracted from the current is used as input data for the fault diagnosis model. The DBN is first trained with the original currents, and then the gradual extraction of the fault characteristic is performed through the multilayer structure. Their results showed that the model can extract the fault feature from the MBS operating currents and implement fault diagnosis effectively, and conclude that the feature extraction effect of this method is better than the traditional feature extraction method and the model has higher diagnostic accuracy.

There are options on the market for monitoring the temperature of the windings of the MBS, among the most important we can mention the Grunfos protection, MP 204 [15], Amacontrol from KSB [16] and Submonitor Connect from Franklin Electric [17], all of them require the invasion of the motor by having to install in the windings of a PT 100 temperature sensor and wire it to the surface, the objective of this work is to propose a protection system based on the normal temperature limit of the motor transmitting the information by current carrier from the

ISSN: 2594 - 2905

MBS to its starter without the need for additional conductors to the power supply (CBS).

DEVELOPMENT
Methodology.

Figure 1 shows the design of the MBS temperature protection system consisting of 5 stages described below:

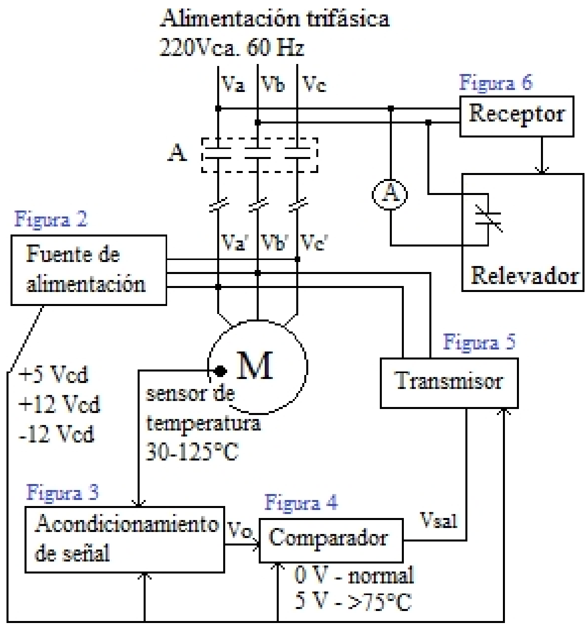

Figure 1. Block diagram.

The design consists of developing a power supply from the motor power supply to supply DC voltage to the electronic circuits. The temperature sensor is connected to a signal to amplify the voltage supplied by a thermocouple so that between 30 and 125°C from an output voltage of 0 to 5V, this is compared with a reference level equivalent to 75°C at which the MBS is protected, If the temperature exceeds the value, it sends 5V to the transmitter to generate a frequency of 200kHz which is injected as a carrier in the power supply conductors. When detected by the receiver, it activates the relay that disconnects the motor power contactor and prevents its connection until the motor cools down. Each module is described in the following sections.

a) Power supply (220VAC/+5, ±12VDC).

The MBSs are powered with three-phase voltages of 440 or 220 volts AC, 60 Hertz without neutral, because this is the only way to ensure that the MBSs can be used in a wide range of applications.

The protection will not have any auxiliary cable, a source was developed with Zener diodes as voltage regulators, to feed the circuits with voltages of +5 and ±12 volts DC.
The power supply will feed three circuits with different voltages and loads, which are shown in Table 1.

Table 1. Load to be fed by voltage.

Cargo	Integrated circuit	Voltage (volts)	Maximum current (mA)
Conditioning	INA 114	± 12	3
Comparator	LM311	+5	7.5
Transmitter (VCO)	MC 4046B	+5	40

The circuit designed for the source is shown in Figure 2.

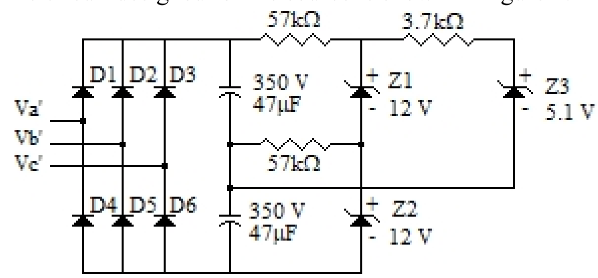

Figure 2. Power supply.

The ±12V DC voltage is obtained with Zener diodes Z1 and Z2 whose parameters are:

$V_{Z1}= V_{Z2}= 12$ V, $P_D= 0.5$ W and $I_{Zmin}= 0.001$ A

The maximum value of the power supply, V_{Smax}, is obtained as a function of the peak phase voltage Vm with equation 1.

$$V_{Smax}= 1.645\ mV \qquad \text{Eq. (1)}$$

Substituting, $V_{Smax}= 1.645(220)= 361.9$ V

Since both positive and negative voltages are needed, a center tap is used to apply half of the voltage to each Zener diode (VZ) and take the center as the neutral of the circuit, therefore:

$$VSmaxZ= 361.9/2= 180.95 \text{ V}$$

The limiting resistance R_i is determined by the load current $IZMAX$, using the equation:

$$Ri= (VSmaxZ- VV)/(1.1\ IZZMAX) \qquad \text{Eq. (2)}$$

Substituting the values into Equation 2 and adjusting to the next higher one defines *Ri* at 57 kΩ.

The power dissipated (*P*) by the resistor is obtained from the current (*I*) by means of:

$$P= I^2{}_{Ri} \qquad \text{Eq. (3)}$$

Substituting the values in equation 3, we obtain a P=0.513 W so a resistance of 1W is required.

It is verified that the maximum power at the Zener diode ($_{PDZ1}$) is not exceeded as a function of Minimum source voltage ($VVSmiin$) and minimum load current ($ILmin$) by means of:

$$_{PDZ1} = \frac{VSmin-VZ}{Ri-ILmin}{}_{VZ} \qquad \text{Eq. (4)}$$

Substituting the values we obtain $_{PDZ1}$= 0.0355W. Therefore, a ½ watt Zener diode is selected.

For the +5V DC source, according to Table 1, a total current of 47.5 mA is used, the values for the Zener diode 3 ($_{Z3}$) are obtained, having the following parameters.

$_{Vz3}$= 5.1 V, PD= ½ W and $_{IZmin}$= 0.001 A.

Substituting the values in Equation 2, the value of the limiting resistance for Zener diode 3 is obtained, the immediate upper $_{Riz3}$ of 3.7 kΩ is considered.

Substituting the values in equation 3, *P= (0.0475)²* * *3,700;* a *P=8*.348 W is obtained, so a 10W resistor is required.

The power of Zener diode 3 is obtained with equation 4 leaving $_{PDZ3}$ = 0.2423 W.

b) Signal conditioning.

The connections for the INA 114 instrumentation amplifier are shown in Figure 3.

The gain (*G*) that can be obtained from NAI 114 is 1 to 10,000 and is controlled by an external resistor, $_{RG}$, the gain is calculated by equation 5.

$$G = 1 + (50\ k\Omega)/RG \qquad \text{Eq. (5)}$$

By subtracting $_{RG}$ from equation 5, we have equation 6.

$$_{RG}= 50(G-1) \qquad \text{Eq. (6)}$$

The thermocouple values were obtained in millivolts, with the help of a digital thermometer ENSA Electronics brand calibrated by CIATEQ and measuring the voltage values in each reading with a digital multimeter Fluke brand calibrated by LAPEM, four readings were taken in a range from 30 to 125 °C, which are shown in Table 2.

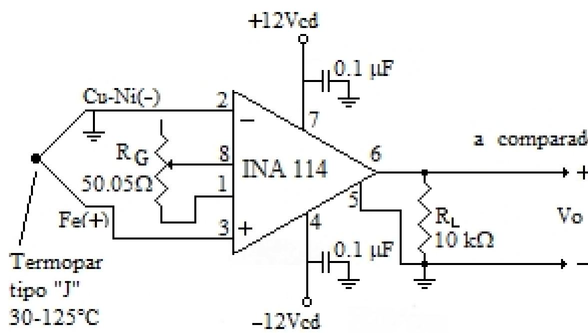

Figure 3. Signal conditioning circuit.

Thermocouple voltages.

Temperature (°C)	Thermocouple voltage (mV)
30	0
75	2.3
100	3.7
125	5

It was decided to take this range since the output voltage at 125 °C is 5 mV, so it is necessary to condition the signal by increasing it a thousand times to obtain an output value (*Vo*) in the range of 0 to 5V; therefore, *G*= 1000.

Equation 6 gives *RG = 50.05Ω;* a precision potentiometer is used to give the exact value.

Graph 1 shows the response of the amplifier for a temperature (*T*) from 0 to 125°C. Using the equation of the line the output function is defined:

$$Vo= (5/95)\ (T - 30)$$

For a value of *T= 75 °C*, we have a value of *Vo*= 2.36 V, this voltage value will serve to place the reference voltage level (*Vref*) in the comparator circuit, *Vo* is greater than this value the comparator will give a high output to activate the transmitter.

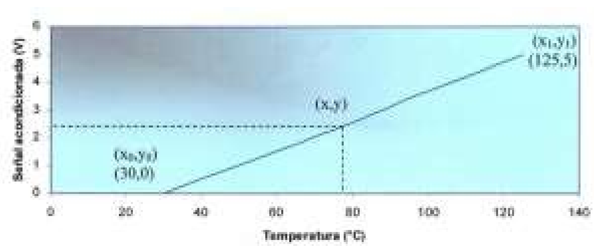

Graph 1. Temperature VS INA 114 output voltage.

c) Comparator.

The LM 311 integrated circuit was used for the comparator, compares a voltage signal at one input with respect to a reference voltage at the other input.

To avoid noise problems, positive feedback is used, it is performed by taking a fraction of the output voltage V_{sal} and applying it to the positive (+) input. In Figure 4, the output voltage V_{sal} is divided by R and n times its value. The input voltage, which comes from the signal conditioning is applied across the resistor R to the (+) input, so the circuit is non-inverting.

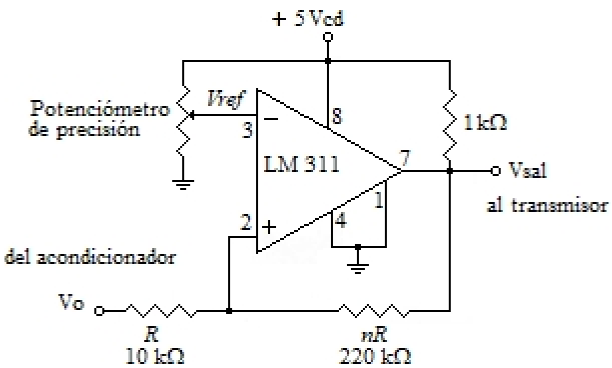

Figure 4. Comparator circuit.

Whenever a circuit changes from one state to a second state with a certain signal and then returns from the second state to the first state with a different input signal, the circuit is said to exhibit hysteresis, therefore, the upper (V_{UT}) and lower (V_{LT}) threshold voltages can be found by the following:

$$V_{U}= Vref\left(+\frac{1}{n}\right)-\frac{-Vsat}{n} \qquad \text{Eq. (7)}$$

$$V_{LT} = Vref\left(1+\frac{1}{n}\right)-\frac{+Vsat}{n} \qquad \text{Eq. (8)}$$

V_{UT} is considered at 2.36 V which corresponds to the temperature limit at 75°C. The comparator is powered at its positive terminal with +5 volts ($+V_{sat}$) and on its positive terminal with $+Vsat$.

negative for 0 volts ($-V_{sat}$), for convenience we define $n=22$ and $R=10$ kΩ, therefore nR= 220 kΩ, Vref is cleared from equation 7 and the values are substituted:

$$Vref= \frac{2.36}{\left(1+\frac{1}{22}\right)} - 0 = 2.26 \text{ V.}$$

Taking the value of V_{ref} and using equation 8, the V_{LT} is calculated:

$$V_{LT} = 2.26\left(1+\frac{1}{22}\right) - \frac{5}{22} = 2.13 \text{ V}$$

Using Equation 7, with $Vo = V_{LT} = 2.13$ V, T is cleared, to know at what temperature value in °C this value represents, with these values we have:

$$T= \frac{95(2.13)}{5} + 30 = 70.47°\text{C}.$$

With this hysteresis range the protection ensures that after the protection is activated the motor will not operate if the temperature does not drop below the V_{LT} value, i.e. 70.47 °C, which is the appropriate temperature for the motor to operate safely.

d) Current-carrier transmitter.

This current-carrier transmitter consists of two parts, a voltage-controlled oscillator (VCO) and a transmitter. The VCO produces an output signal, generally a square wave, whose frequency is proportional to the value of a DC voltage applied at its control input.

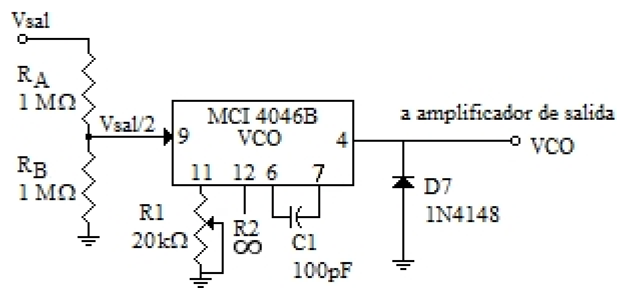

Figure 5. Transmitter circuit.

The comparator signal enters the VCO of the Phase-Locked Loop (PLL) of the circuit.
MC1 4046B, which is responsible for modulating the incoming signal on a 200 kHz carrier, the minimum frequency (f_{min}) can be determined by the equation 9 and the maximum frequency (f_{max}) is calculated with the

Equation 10, for this application it is not required to shift the center frequency so f_{min} is zero Hertz, from equation 9, *R2* is∞ ; pin 12 is disconnected.

$$f_{min}= \frac{1}{R2(c1+32pF)} \qquad \text{Eq. (9)}$$

$$f_{max}= \frac{1}{R1(c1+32pF)} \qquad \text{Eq. (10)}$$

Considering an f_{max}= 400 kHz, the capacitor is defined as follows
C1=100 pF and from equation 10 we calculate the value of *R1*
= 18,939.39; it is selected at 20 .

The VCO operates at a specific frequency, called center frequency (F_0); defined by the input voltage coming from the comparator. The voltage divider is set with RA and RB, defined at 1 MΩ. When the comparator signal is high (5V), at the input applies *Vsal/2* then the center frequency is:

$$F_0 = fmax/2 \quad \text{Eq. (11)}$$

With f_{max}= 400 kHz substituting the value in equation 11 gives the value of F_0 = 200kHz.

The VCO output is 5V; this signal is amplified by the PN 2222 A transistor, the equation of the right-hand side mesh shown in Figure 6 is:

$$I_C\,(R_{CE}+R4)+V_{CE}=12 \quad \text{Eq. (12)}$$

Where I_C is the collector current, R_{CE} is the equivalent collector resistance, *R4* is the emitter resistance and V_{CE} is the collector-emitter voltage.

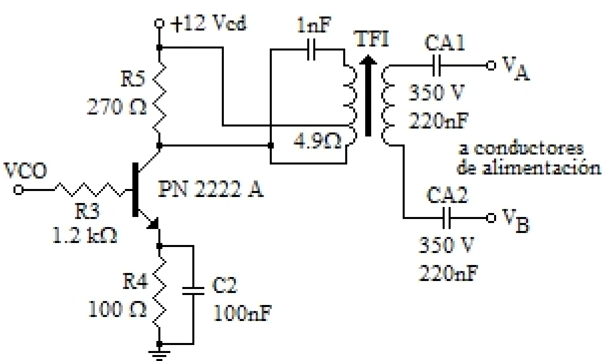

Figure 6. Amplification of the VCO output signal.

The equivalent collector resistance (ECR) is calculated from the resistance *R5* and the resistance of the intermediate frequency transformer (IFT) *RT2*:

$$R_{CE} = \frac{R5 * RT2}{R5 + RT2} \quad \text{Eq. (13)}$$

For the mesh on the left side, in Figure 6, the equation is defined by:

$$I_B R3 + V_{BE(satt)} = 5 \quad \text{Eq. (14)}$$

Where: I_B is the base current, *R3* is the base resistance and $VBE_{(sat)}$ is the base-emitter voltage at saturation.

The base current is defined from the transistor gain (β) by:

$$I\_B = IC/\beta \quad \text{Eq. (15)}$$

This amplified signal is placed on the TFI transformer operating up to 455 kHz for injection into the power grid. The TFI must be synchronized to the carrier frequency of 200 kHz. Capacitors CA1 and CA2 shown in Figure 6 are high voltage and isolate the TFI transformer from the mains.

The PN2222A transistor has the following parameters in its data sheet, $VCE_{(sat)}$ = 1 V, $VBE_{(sat)}$ = 2 V and β = 40.

We define *R5* = 270Ω and R4 = 100Ω; using a digital multimeter we obtain the resistance value of the TFI =.9Ω. Substitute the values in equation 13 to obtain R_{CE} = 4.81Ω.

Equation 12 is used to calculate the collector current I_C = 0.1049 A. Equation 15 gives the value of I_B:

$$I_B = 0.1049/40 = 2.623\times10^{-3}\ \text{A}$$

using equation 14, *R3* is cleared to obtain its value; *R3*= 1.143, it is set at commercial value of 1.2 kΩ. The transmitter circuit is shown in Figure 6 with the design values.

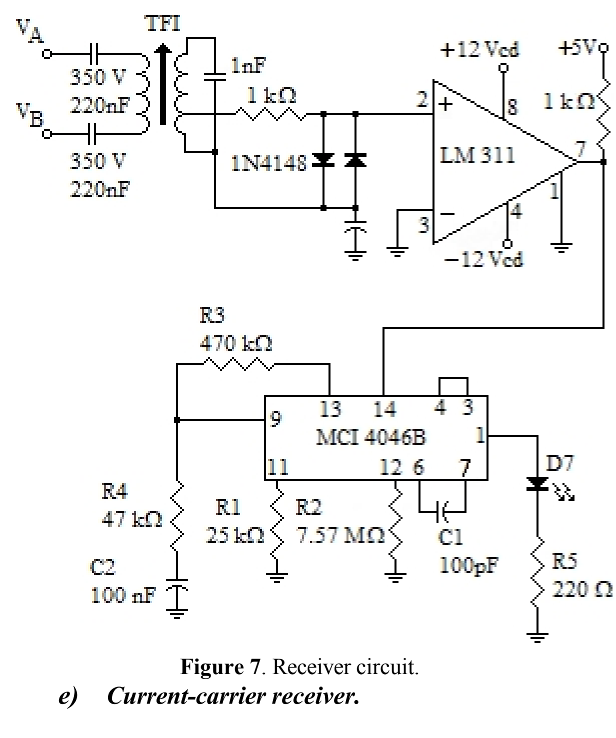

Figure 7. Receiver circuit.

e) *Current-carrier receiver.*

The signal coming from the mains should be isolated by two high voltage capacitors and inserted into a TFI of the same characteristics as the transmitter, as shown in figure 7.

EDUCACIÓN TECNOLÓGICO NACIONAL DE MÉXICO
IPSUMTEC
ISSN: 2594 - 2905

The signal provided by the TFI is amplified by means of a voltage comparator LM311, a pull up resistor of 1 kΩ is placed at its output a voltage of 5 Vpp with a frequency of 200 kHz is obtained
The TFI must be synchronized at 200 kHz, which is the carrier frequency used for signal transmission, which can be recovered at distances greater than 10 m, by means of a receiver such as the one shown in Figure 7, based on a PLL, which is a frequency control system consisting of a comparator or phase detector, a low-pass filter and a VCO. This stage is developed with the 4046B integrated circuit that includes the three elements.

The PC2 comparator is used, which is known as a broadband phase detector because it has a much wider capture range and accepts asymmetrical input signals. The input signal is applied to pin 14 (SIGNAL IN) and the comparison signal from the VCO (pin 4) is applied to pin 3 (COMP IN).

This comparator delivers at its output (pin 13) a high level when the input frequency is higher than that of the VCO and a low level in the opposite case. If the 2 signals have the same frequency and phase, the output of the control pin 1 (PHASE PULSES), becomes high, this information is used to indicate to the external circuits that the PLL is latched; in this case it activates the relay shown in figure 1 to de-energize the motor.

Resistors R3, R4 and C2 form a low-pass filter, which determines the rate at which the system can follow changes in input frequency, the capture range and prevents the normal operation of the PLL from being affected by noise peaks.

For the receiver, the offset level was increased to 10 kHz. C1 is defined at 100 pF and using equation 9 calculates R2 obtaining a value 7.57 MΩ. This prevents it from latching to the 60 Hz power line frequency.

The maximum frequency (f_{max}) was set with a value of 300 kHz, with equation 10, the value of R1 at 27 kΩ is obtained.

The PLL system latching range (Δ_{FL}), defines the frequency band within which the PLL can be kept latched with a previously captured input signal. It is evaluated by:

$$\Delta_{FL} = \pm(fmax - fmin)/2 \qquad \text{Eq. (18)}$$

The capture range of the system itself (Δ_{FC}), defines the frequency band within which the PLL can track and capture an input signal until it latches on with it. Since the PC2 comparator (pin 13) was used, the capture range will be equal to the latching range, i.e:

$$\Delta_{FC} = \Delta_{FL} \qquad \text{Eq. (19)}$$

Therefore, the PLL will be able to capture and stay on-hook with any frequency within the operating range of the VCO.

The protection is calibrated and adjusted for testing at a distance of 13.5m.

DISCUSSION AND ANALYSIS OF RESULTS

Figure 8 shows the carrier signal, which is obtained by increasing the temperature to a value higher than 75°C.
°C, achieving a 5 Vpp signal at a frequency of 200 kHz.

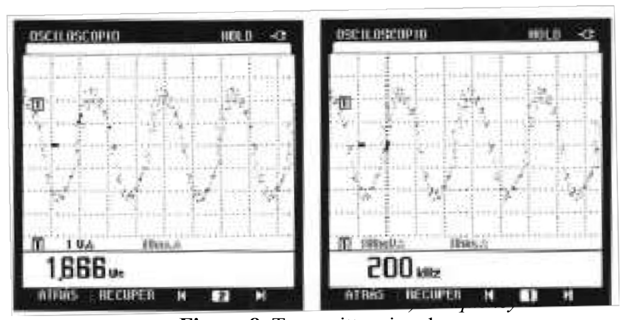

Figure 8. Transmitter signal.

Figure 9 shows how this 200 kHz carrier signal is mounted on top of the 60 Hertz feed signal, making it look a little wider and increasing its amplitude.

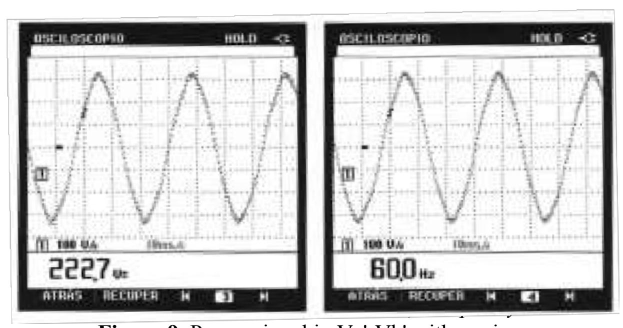

Figure 9. Power signal in Va'-Vb' with carrier,

In Figure 10, a close-up of the feed signal with the carrier around 200 kHz can be seen.

The receiver circuit was placed at the opposite end of the 13.5m Submersible Pump Cable, filtering the 200 kHz carrier signal generated by the transmitter, the signal at the output of the transmitter is shown in Figure 11.

TFI, with the drawback of its small amplitude device triggering; about 1 Vpp.

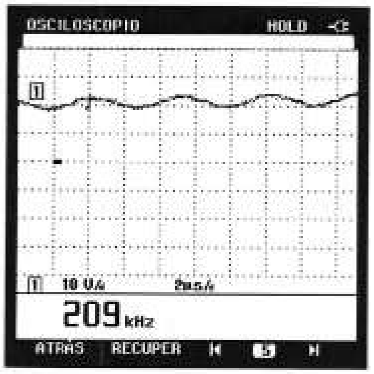

Figure 10. Va'-Vb' feed signal with extended carrier.

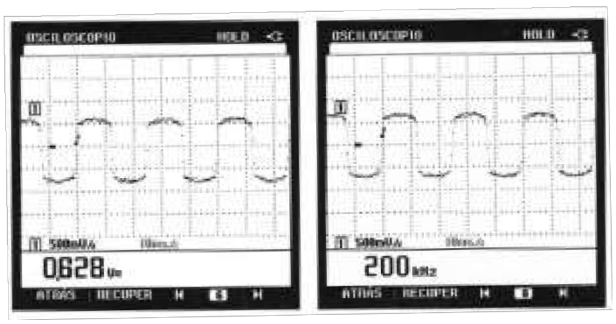

a) Voltage *b) Frequency*

Figure 11. TFI output signal from the receiver

The LM311 comparator is used to convert the signal to digital from 0 to 5 V; the response is shown in Figure 12:

a) Voltage *b) Frequency*

Figure 12. Signal at the output of the LM311.

This signal is inserted into the PLL at its pin 14 (SIGNAL IN), to compare it with the VCO signal and as it falls within the latching range of 10 to 300 kHz the system was successfully latched, as shown in Figure 13.

Finally, the engine was allowed to cool down, reaching room temperature, i.e. with the lowest temperature of the engine.

at 70 °C, the output was set to low, 0 V, as shown in Figure 14.

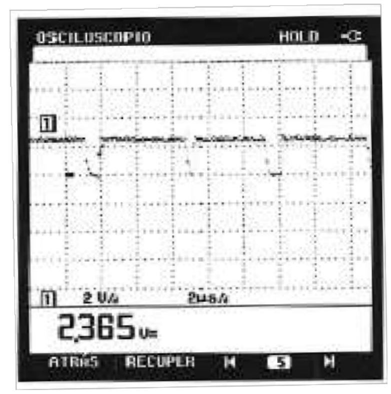

Figure 13. Pin 1 output high, receiver voltage latched.

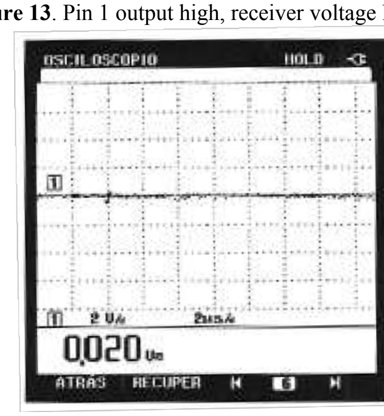

Figure 14. Low output, no voltage at the receiver.

Although in [13] they concluded that the proposed system is simple and economical, as well as reliable, there is still the inconvenience of having to wire the three sensors from the MBS to the surface, something that is eliminated with this proposal by sending the signal by current carrier.

The designed protection unlike [14] does not need prior fault information for learning the neural network, only the maximum operating temperature of the MBS needs to be selected for the protection to act.

The main advantage of this proposal compared to [15], [16] and [17] is its universality since it can be fitted to any type of MBS, of any brand and of any capacity in any submersible pump repair shop so it is not limited to certain brands or capacities of MBS.

CONCLUSIONS

It can be concluded that the carrier temperature protection uses the supply conductors for communication between the sensor and the actuator. The high temperature warning signal is generated at 75°C. When the temperature drops to a value of 70°C the output is deactivated allowing the pump to operate again. Hysteresis operation is achieved, ensuring that the motor can operate safely when it has cooled down. The proposed system protects the motor by preventing it from exceeding the normal operating temperature without the need for additional wiring to the power supply. This alert indicates that maintenance is required, and when done in a timely manner, the cost of repair is reduced.

Future research is to work on the evaluation of the insulation degradation from the temperature increases registered in the pump to predict the failure before it occurs. Another field research is to develop an algorithm that allows the self-calibration of the transmission of information by carrier as a function of the depth of the submersible pump.

ACKNOWLEDGMENTS

Special thanks to the Instituto Tecnológico de Aguascalientes for the facilities for the use of materials and the use of the Electrical Engineering laboratory.

BIBLIOGRAPHY .

[1] Villalobos-Piña, F. J., & Álvarez-Salas, R. (2015). Robust algorithm for the diagnosis of electrical faults in three-phase induction motor based on spectral and ondelta tools. Revista Iberoamericana de Automática e Informática industrial, 12(3), 292-303. doi:https://doi.org/10.1016/j.riai.2015.04.003

[2] Barrios Castellanos, M., Serpa, A. L., Biazussi, J. L., Monte Verde, W., & N.S., D. A. (January 2020). Fault identification using a chain of decision trees in an electrical submersible pump operating in a liquid-gas flow. Journal of Petroleum Science and Engineering, Volume 184(106490). doi:https://doi.org/10.1016/j.petrol.2019.106490

[3] Tahmasebi, P., Kamrava, S., Bai, T., & Sahimi, M. (August 2020). Machine learning in geo- and environmental sciences: From small to large scale.(ELSEVIER, Ed.) Advances in Water Resources, Volume. 142(103619). doi:https://doi.org/10.1016/j.advwatres.2020.103619

[4] Wei, Q., Sun, X., & Y., S. A. (September 12, 2019). Numerical study on the impact of the coupling of diffuser parameters on the performance of submersible pumps used in town water distribution systems. Journal of the Brazilian Society of Mechanical Sciences and Engineering , Volume 41(article number 408). doi:https://doi.org/10.1007/s40430-019-1911-8

[5] Peng, Y., Ye, C., Sun, F., Wang, X., Zhu, P., Zhu, Q., . . . Wang, W. (October 2018). Drainage gas recovery technology for high-sulfur gas wells by a canned ESP. system. Natural Gas Industry B, Volume 5(Issue 5), Pages 452-458. doi:https://doi.org/10.1016/j.ngib.2018.02.002

[6] Pezzuto, A., & Sarver, E. (October 2020). A lab study of mineral scale buildup on line and traditional PE water pipes for acid mine drainage. Journal of Sustainable Mining, Volume 19(Issue 1), 31-45. doi:http://dx.doi.org/10.46873/2300-3960.1004

[7] Kox, T., Lu¨der, C., & Gerhold, L. (March 12, 2018). Anticipation and Response: Emergency Services in Severe Weather Situations in Germany. International Journal of Disaster Risk Science , Volume 9, pages 116-. 128. doi:https://doi.org/10.1007/s13753-018-0163-z

[8] Bellini, A., Filippetti, F., Tassoni, C., & Capolino, G.-A. (December 2008). Advances in Diagnostic Techniques for Induction Machines. IEEE TRANSACTIONS ON INDUSTRIAL ELECTRONICS, 55(12), 4109 - 4126. doi:https://doi.org/10.1109/TIE.2008.2007527

[9] Garcia-Guevara, F. M., Villalobos-Piña, F. J., Alvarez-Salas, R., Cabal-Yepez, E., & Gonzalez-Garcia, M. A. (2016). Stator Fault Detection in Induction Motors by Autoregressive Modeling. Mathematical Problems in Engineering, Volume 2016(Article ID 3409756), 7 pages. doi:http://dx.doi.org/10.1155/2016/3409756

[10] Al-Hashmi, S. A. (March 2021). Condition monitoring of Electrical Submersible Pumps (Faults review). Journal of Pure & Applied Sciences, Vol. 20(No. 1), 71-74. doi:http://dx.doi.org/10.51984/jopas.v20i1.1070

[11] Fink, D. G., & Wayne Beaty, H. (1996). Handbook of Electrical Engineering (Vol. VOL. VOL. I). (J. H. Romo Muñoz, R. García Díaz, J. H. Pérez Castellanos, J. De la Cera Alonso, J. R. Salas Contreras, & E. Ramírez Grycuk, Trads.) McGRAW-HILL. doi:ISBN 970-10-0872-3

[12] Oliveira-Santos, T., Rauber, T., Varejão, F., Martinuzzo, L., Oliveira, W., Pellegrini Ribeiro, M., & Rodrigues, A. (November 06-08, 2016). Submersible Motor Pump Fault Diagnosis System: A Comparative Study of Classification Methods. (IEEE, Ed.) 2016 IEEE 28th International Conference on Tools with Artificial Intelligence (ICTAI), 415 - 422. doi:https://doi.org/10.1109/ICTAI.2016.0070

[13] Sanad, K. A., El-Samahy, A. A., & Mourad, D. (May 1, 2022). Performance Analysis and Protection of Submersible Motor for Unbalance Condition in Dewatering. (N. S. Cor., Ed.) International Journal of Thin Films Science and Technology, 11(No. 2), 191-199. doi:http://dx.doi.org/10.18576/ijtfst/110206

[14] Yu, D., & Zhang, H. (June 15, 2020). Fault Diagnosis Method for Submersible Reciprocating Pumping Unit Based on Deep Belief Network.(IEEE, Ed.) IEEE Access, Volume: 8, 109940 - 109948. doi:https://doi.org/10.1109/ACCESS.2020.3002376

[15] Grundfos Mexico (n.d.). Grundfos. Retrieved April 15 April from 2024, from https://product-

selection.grundfos.com/mx/products/mp/mp-204/mp-204-96079927?pumpsystemid=2361219131&tab=variant-specifications
[16] KSB de México, S.A. de C.V. (n.d.). KSB. Retrieved April 15, 2024, from https://www.ksb.com/es-es/lc/productos/automatizacion- de-bomba/amacontrol/A75B
[17] Franklin Electric Latin America. (n.d.). franklinagua.com. Retrieved April 15, 2024, from https://franklinagua.com/productos/arrancadores,-controls-and-protections/components-for-controls-and-protections/trif%C3%A1sic-protections-submonitor-connect.aspx.

CONTRIBUTION ROLES

Role	Author(s)
Project conceptualization and management.	Oscar Manuel Cortés
Data curation and monitoring	Mario Salvador Esparza Gonzalez
Methodology	Christian Geovanni Hernández Murillo